



Comparative study of arsenic toxicosis and ocular pathology in wild muskrats (*Ondatra zibethicus*) and red squirrels (*Tamiasciurus hudsonicus*) breeding in arsenic contaminated areas of Yellowknife, Northwest Territories (Canada)

S. Amuno^{a,*}, L. Bedos^b, V. Kodzhahinchev^c, K. Shekh^{c,d}, S. Niyogi^{c,d}, B. Grahn^b

^a School of Environment and Sustainability, University of Saskatchewan, Saskatoon, Canada

^b Western College of Veterinary Medicine, University of Saskatchewan, Saskatoon, Canada

^c Department of Biology, University of Saskatchewan, Saskatoon, Canada

^d Toxicology Centre, University of Saskatchewan, Saskatoon, Canada

HIGHLIGHTS

- Retina layer changes were assessed in two wildlife species from As endemic areas in Canada.
- Thicknesses of several retinal layers were reduced in muskrats but not in squirrels.
- The high incidence of ocular abnormalities and visual dysfunction in muskrats could be a concern for wildlife exposed to As.

ARTICLE INFO

Article history:

Received 5 November 2019

Received in revised form

20 January 2020

Accepted 21 January 2020

Available online 25 January 2020

Handling Editor: Willie Peijnenburg

Keywords:

Arsenic poisoning

Metal exposure

Ocular pathology

Retina changes

Cognitive impairment

And wildlife population

ABSTRACT

The Giant Mine is an abandoned gold mine in Yellowknife, Northwest Territories, Canada. Throughout its operation from 1948 to 2004, the Giant Mine released heavy amounts of arsenic trioxide into the environment, thus contaminating the soil and surface water within and around the vicinity of the mine site. Chronic arsenic (As) poisoning negatively impacts wildlife health and can induce multi-organ damages including neurodegeneration and visual dysfunction depending on concentration and duration of exposure. The aim of the current study was to comparatively assess retina layer changes and prevalence of ocular lesions in wild rodent populations (i.e. muskrats and red squirrels) breeding in arsenic endemic areas of Yellowknife, near the vicinity of the abandoned Giant mine site (~2 km radius), at an intermediate location (approximately 20 km from the mine area) as well as a reference location (spanning 52–105 km from the city of Yellowknife, Canada). Eye globes were removed from euthanized muskrats and squirrels from the three sampling locations with increasing distance from the Giant mine area. Optical Coherence Tomography (OCT) was used to attempt a pan-retinal layer assessment, and histologic examination was utilized for assessment and confirmation of ocular lesions. The retinal layers were measured and statistically compared between the groups based on sampling locations to enhance the scope of histologic evaluations. The preliminary results revealed that thicknesses of ganglion cell layer (GCL), retina nerve fibre layer (NFL), and inner retina layer (IR) were statistically reduced in the muskrats from arsenic endemic area, particularly near the vicinity of the Giant mine compared to the control group. Generalized ocular pathology was histologically confirmed in all the muskrats from the arsenic endemic areas with the manifestation of moderate to severe lymphocytic plasmacytic uveitis (LPU), keratitis and subcapsular cataracts. Inner retinal degeneration was also observed in all the muskrats from the arsenic endemic areas, while muskrats from the control group were predominantly normal. Three muskrats from the control group were noted to have a mild LPU and keratitis. Significant histopathologic changes were not detected in the squirrel eyes from the three groups except for incidental mild cornea scars from all the locations. In general, these preliminary findings confirm the presence of ocular lesions and retina abnormalities in wild muskrats in the Yellowknife area and provide

* Corresponding author.

E-mail address: soa882@usask.ca (S. Amuno).

the first evidence of visual dysfunction and impairment in wildlife inhabiting arsenic endemic areas of Canada.

© 2020 Elsevier Ltd. All rights reserved.

1. Introduction

Previous gold mining and arsenopyrite ore roasting activities at the Giant Mine site (1948–2004) resulted in the emission of high amounts of arsenic and other trace metals into the terrestrial and aquatic ecosystems of Yellowknife, Northwest Territories, Canada. Among all the emissions from Giant Mine, arsenic is the metalloid of most significant environmental concern because the emission levels of arsenic were extremely high when the mine was operational (Clark and Raven, 2004). Elevated levels of arsenic have been consistently reported in surface soils, vegetation and lakes near the vicinity of the Giant mine area and in surrounding locations near the City of Yellowknife (Amuno et al., 2018; Bromstad et al., 2017; Cott et al., 2016; Fawcett et al., 2015; Government of Northwest Territories, 2016; Hutchinson et al., 1982; Wagemann et al., 1978). It should be noted that after the closure of the Giant mine in 2004, the responsibility for care and maintenance of the mine fell on the Government of Canada to address the environmental legacy issues left behind by the mine operators, particularly the 237,000 tonnes of arsenic trioxide dust currently stored in underground frozen chambers at the Giant Mine site (“Giant Mine Remediation Project”, 2017). Currently, remediation activities are being undertaken to secure the frozen underground arsenic trioxide waste containment area at the Giant Mine site.

Studying the adverse effects of chronic arsenic poisoning in small mammals could be highly useful for risk assessment and management of contaminants because small mammals can act as sentinels for environmental contamination (O'Brien et al., 1993). In addition, data from small mammals could provide important information about the threats from contaminants to other organisms that share the same environment as humans (O'Brien et al., 1993). Small mammals such as snowshoe hares living near the vicinity of Giant Mine have been shown to accumulate higher levels of arsenic (Amuno et al., 2018). Small mammals such as Wild Muskrats (*Ondatra zibethicus*) and Red Squirrels (*Tamiasciurus hudsonicus*) are commonly found in Northwest Territories of Canada, including Yellowknife (D'Entremont, 2014; Banfield, 1951); however, the pathophysiological impact of chronic exposure to high environmental levels of arsenic has not been assessed in detail in these species to date. Although some of the previous studies have investigated oxidative stress and neurotransmission biomarker responses in brain (Amuno et al., 2019a, 2019b) currently there is no information on arsenic induced ocular biomarkers in these species.

Chronic arsenic exposure has been identified as a potential risk for neuropathy, cognitive impairment and neurological disorders in both human and animal models (Kobayashi and Agusa, 2019). Several well-defined neurodegenerative diseases such as Alzheimer Disease (AD), Dementia, Multiple Sclerosis (MS) and Parkinson's disease (PD) that affect the brain and spinal cord have manifestations in the eyes (Iranzo et al., 2006), and ocular symptoms often precede conventional diagnosis of such central nervous system (CNS) disorders (Jefferis et al., 2011). The etiology of these diseases is still unclear; however, several studies have confirmed that exposure to neurotoxic metal(loids) such as arsenic may increase beta-amyloid peptide and the phosphorylation of Tau protein, and neuronal death. Since arsenic is widely present in the

environment due to geogenic contamination and anthropogenic activities (i.e. mining), wildlife and human population around those areas may be susceptible to chronic arsenic poisoning which may induce neurodegenerative pathology. Since the retina is a developmental outgrowth of the brain and is known to share many features with the brain including embryological origin, anatomical and physiological characteristics, alteration of retina layers have been used as an ocular biomarker for diagnosing and monitoring the progression of various neurologic diseases in human and animal studies (London et al., 2013; Ikram et al., (2012). Studies have shown that alteration of retina layers can reliably provide an easily accessible and non-invasive way of examining the pathology of the brain (Chan et al., 2017). In addition, there is also growing evidence that the visual system is also involved in several neurodegenerative diseases (McKeith et al., 2005; Fisher et al., 2006). For example, visual loss is a major symptom amongst patients with MS, and some degree of visual impairment develops along the course of the disease (Miller et al., 2005; Karussis, 2014; Dobson and Giovannoni, 2019).

Several studies have shown that ocular abnormalities associated with cognitive deficits are linked with nerve fibre layer thinning (Kesler et al., 2011), degeneration of the retinal ganglion cells (Shentu et al., 2019), and changes to ocular vascular parameters (Jung et al., 2019). Furthermore, microcystic macular edema and associated thickening of the retina inner nuclear layer was found to represent markers of active CNS inflammatory activity (Costello and Burton, 2018). In patients with multiple sclerosis (MS) for example, retina nerve fibre layer (NFL) thickness correlates directly with progression of neurological impairment and with disease duration (London et al., 2013). The study by Parisi et al. (1999) noted a significant reduction in NFL in patients with MS compared to healthy subjects. Saidha et al. (2011) also observed significant retina ganglion thinning in patients with relapsing remitting and progressive MS. There have been several studies reporting NFL thinning and decreased macular volume in PD patients compared to control healthy subjects (Satue et al., 2016; Kwapong et al., 2018). Aside from retina layer changes, several ocular lesions such as lens opacification, uveitis and other visual impairments are also associated with cognitive impairments and demyelinating diseases of the CNS (DeSousa et al., 2002; Fukuoka et al., 2015). Despite the well documented pattern of retina changes in human and animal models of neurodegeneration, our understanding of how chronic arsenic exposure induces distinctive neurological disorders and structural changes in the eyes, particularly within the retina of wildlife is still unknown. Since the retina is an extension of the brain embryologically, it can reveal pre-symptomatic evidence of idiopathic dementing diseases and can provide a non-invasive way to examine the pathology of the brain.

In this present study, we hypothesized that wild rodents inhabiting arsenic contaminated areas will carry higher arsenic burden and show evidence of ocular degenerative disease including thinning of retina layers compared to animals inhabiting areas with background levels of arsenic. In addition, despite concerns that chronic As exposure has been associated with neurodegenerative diseases and ocular pathology, no study has specifically investigated retina neurodegeneration and ocular pathology in wildlife species from arsenic endemic areas of Canada. The purpose of this

present study was to investigate whether chronic arsenicosis might induce significant ocular pathology and degeneration of retinal layers in wild muskrat and squirrel populations breeding in arsenic endemic areas of Yellowknife, near the vicinity of the abandoned Giant mine site compared to reference locations away from the city of Yellowknife.

The animals selected for this study are known to have small and limited home ranges and are generally considered suitable for biomonitoring the toxic effects of contaminant exposure. For example, muskrats (*Ondatra zibethicus*) typically have small home ranges of 20 yards or less from their push ups or dens, but they are capable of dispersing long distances to find food or suitable habitats (Woodland Fish and Wildlife, 2015). Red squirrels (*Tamiasciurus hudsonicus*) on the other hand have home ranges that are between 1 and 2.4 hectares (Ruff and Wilson, 1999). Due to the small home ranges of the muskrats and red squirrels, these animals may be susceptible to contaminant exposure as a result of their proximity to polluted areas and may exhibit pathological effects. Prior to this investigation, we previously reported evidence of chronic arsenicosis and the high prevalence altered biochemical parameters and bone abnormalities in wild snowshoe hares breeding near the vicinity of the Giant mine area (Amuno et al., 2018).

2. Material and methods

A wildlife research permit (WLWL500561) and ethical clearance for wildlife handling was obtained from the Department of Environment and Natural Resources, Government of the Northwest Territories as well from the University of Saskatchewan. A general research licence (No. 16190) was also obtained from the Aurora Research Institute prior to commencement of the field study. An experienced local furbearer hunter was employed to assist in determining breeding locations of muskrats and squirrels prior to trapping in the study area.

2.1. Diagnosis of chronic arsenicosis

The diagnosis of chronic arsenicosis in the wild muskrats and squirrels was based on the following assessment:

- (i) Arsenic exposure data: we undertook chemical site characterization of the study area by measuring As and other toxic elements in the surface soil, surface water and vegetation samples which are key components of the habitat for the muskrats and red squirrels and all of these components could be potential source of dietary exposure to metal(oids) in both species. Our previous investigation reported elevated concentrations of As in the soils and vegetation samples from ~2 to 20 km radius of the vicinity of the Giant mine site (Amuno et al., 2018). Both model species, muskrat and red squirrels rely predominantly on the vegetarian diet (Moller, 1983; Stearns and Goodwin, 1941); hence, as mentioned above, plants could be an important source of metal(oid) exposure in these species. In addition, a previous investigation of up to 98 lakes within a 30 km radius of the City of Yellowknife already confirmed that As concentration exceeded the federal drinking water guideline of 10 µg/L for many lakes within 12 km of the Giant mine area (Palmer et al., 2015).
- (ii) Evaluation of chronic As exposure: Evidence of long-term or chronic As exposure was obtained through the measurement of total As levels in the nail samples of muskrats and squirrels from As affected areas and the reference locations. Data pertaining to As levels in the brains and stomach content of

muskrats and squirrels from the study area have been published in (Amuno et al., 2019a, 2019b).

2.2. Animal sampling

Field work took place between March and April 2018 and tissues samples of the squirrels and muskrat were obtained through the legal harvest of a local furbearer hunter in Yellowknife. Squirrels were killed using a 0.20 calibre shot gun, while a drowning set was used for trapping muskrats. The ages of the squirrels and muskrats were estimated based on body weight and length; a squirrel was considered adult (>1year old) if the overall body length was between 10 and 15 inches and weighed between 260 and 350 g (Pennsylvania State University, 2002). A muskrat was considered adult (>1year old) if it weighed between 2.5 and 4 pounds with total body length ranging from 23 to 26 inches and with a tail length of 8–11 inches (New York Department of Environmental Conservation). All the squirrel and muskrats sample utilized for this study generally met the adult criteria.

2.3. Sampling locations

The study aimed to assess animals near the Giant Mine site, a closed gold mine located near the city of Yellowknife, Northwest Territories, Canada. Adult muskrats and red squirrels trapped at either the immediate vicinity of the mine (within ~2 km radius) or at an intermediate location (20 km away from the mine) were compared with animals from a reference site (muskrats and squirrels trapped between 53.4–62 km and 95–105 km away from Yellowknife, respectively; Fig. 1).

2.4. Laboratory analysis

(i) Ocular Pathology:

The eye globes of muskrats and red squirrels were promptly collected from five (5) animals from each sampling location or group (a total of 15 muskrats and 15 squirrels) and immersed in Davidson's fixative solution. Ten globes from muskrats and squirrels collected from the three locations were examined with a light microscope. All globes after a minimum of 48 h of fixation were sectioned and processed for histologic examination similar to previous descriptions (Grahm et al., 2018). Each globe was examined by a veterinary ophthalmologist and was grossly sectioned with a blade in a sagittal plane through the optic nerve and through the cornea to allow examination of the dorsal and ventral ocular tissues. Each half was photographed, and the posterior segment was identified and placed on a mounting pedicle and the retina was examined with optical coherence tomography (OCT). The Heidelberg Spectralis OCT (Heidelberg Engineering, CA, USA) was used to collect retinal nerve fibre layer thickness and retinal measurements aligning the scan to contact the optic nerve. Unfortunately, the smaller size of the globes precluded meaningful optical coherence tomography on either population of these animals. One half of each globe was re-sectioned with the brain blade to remove a cap of sclera, uvea and retina to allow wax penetration through the globe during wax impregnation. The central calotte was then placed in an embedding chamber and wax impregnated and sectioned with a histotome and sections were placed on glass slides and were routinely stained with hematoxylin and eosin and periodic acid Schiff. Slides were examined by a veterinary ophthalmologist who was masked to the groups. The retinal layers of all the squirrels and muskrats were measured histologically from two areas equidistance from the optic nerve (Fig. 2) and these were compared

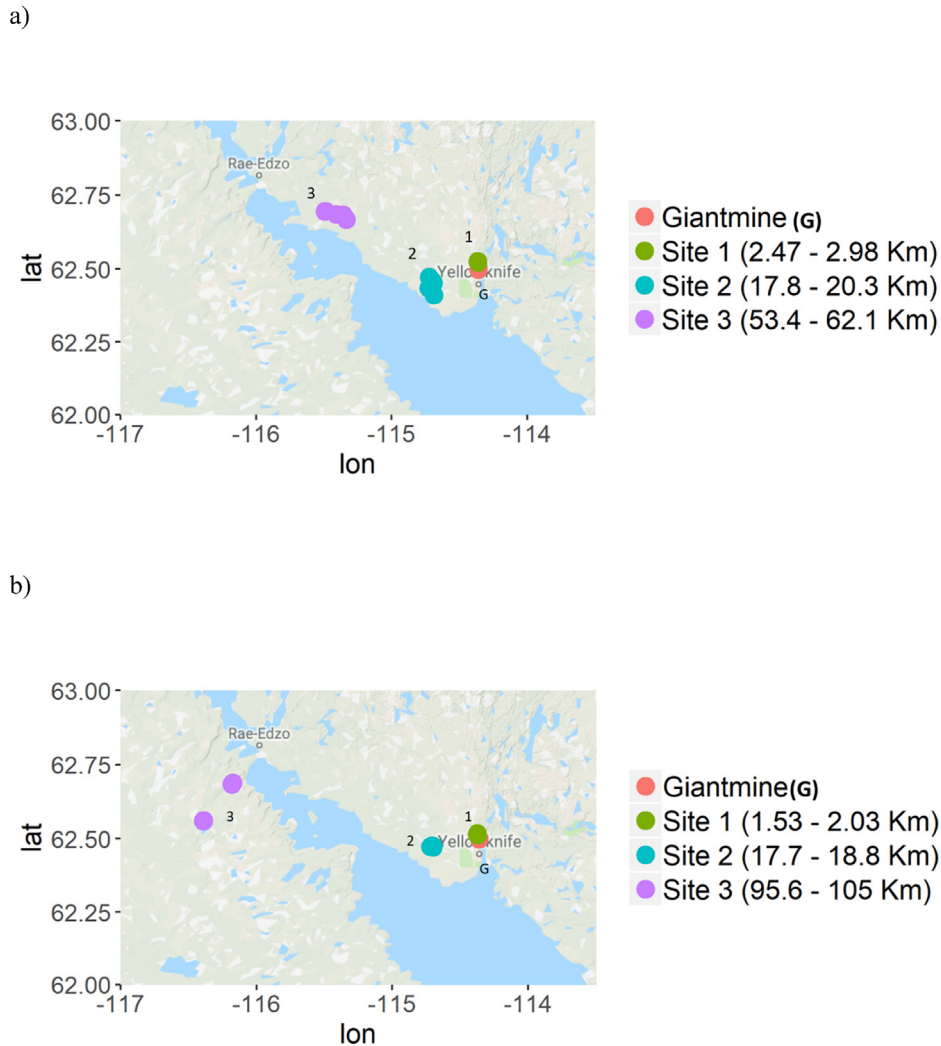


Fig. 1. Map of study area showing specimen collection and mining area. a) Muskrat b) squirrel.

statistically from each area. The following layers were specifically measured: outer nuclear layer (ONL), outer plexiform layer (OPL), inner nuclear layer (INL), inner plexiform layer (IPL), ganglion cell layer (GCL), retina nerve fiber layer (NFL) and inner retina (IR).

(ii) Arsenic and Cadmium Analysis in nails of Muskrats and Squirrels

The nails were digested in polyethylene conical centrifuge tubes for 48 h in 5 vol of 16 N trace metal grade Nitric acid (EMD Millipore, Billerica, MA, USA) at 60 °C in a heating oven. Nails were washed once with deionized water to remove the soil contamination from external surface. After digestion, tissue digests were centrifuged at 2500 g for 10 min and supernatants were collected. The concentrations of As and Cd in supernatants were measured using a graphite furnace atomic absorption spectrometer (AAAnalyst 800, PerkinElmer, USA) after appropriate dilution of samples in 0.2% nitric acid. For quality control and assurance purposes, appropriate method blanks, certified Cd and As standards (Fisher Scientific, Canada), and a reference material (DOLT-4; National Research Council of Canada) were included in the measurements. The recovery percentage of Cd and As in the reference material was 96% and 92%, respectively and the trace metal concentrations in animal tissues were normalised on the basis of wet tissue weight

(Amuno et al, 2018).

(iii) Analyses of Environmental Contamination

Elemental analyses of the study area was determined through the measurement of the total As and Cd in the surface water and soil from samples collected at each of the sites. Moreover, representative vegetation in the study area (e.g. cattail, mushrooms, and blade grass) was also analyzed for As and Cd content because both model species, muskrat and red squirrels rely predominantly on the vegetarian diet (Moller, 1983; Stearns and Goodwin, 1941); hence, plants are expected to be an important source of dietary exposure. The detailed description of the study area with respect to elemental concentrations and the potential wildlife exposure to environmental contaminants were previously reported (Amuno et al., 2018). The soil and plant samples were all shipped to a commercial laboratory (ACME laboratory, Vancouver) for trace element analysis as outlined in Amuno et al. (2018). Soil samples were collected from a depth of up to 20 cm from the study area, and with increasing distance from the Giant mine site. 250 µm of sieved soil samples were analyzed for selected trace metals by ultra-trace inductively coupled plasma mass spectrometry (ICP-MS) following Aqua Regia digestion. 0.5 g of soil sample was digested with aqua regia for 2 h at 95 °C, when cooled the sample was

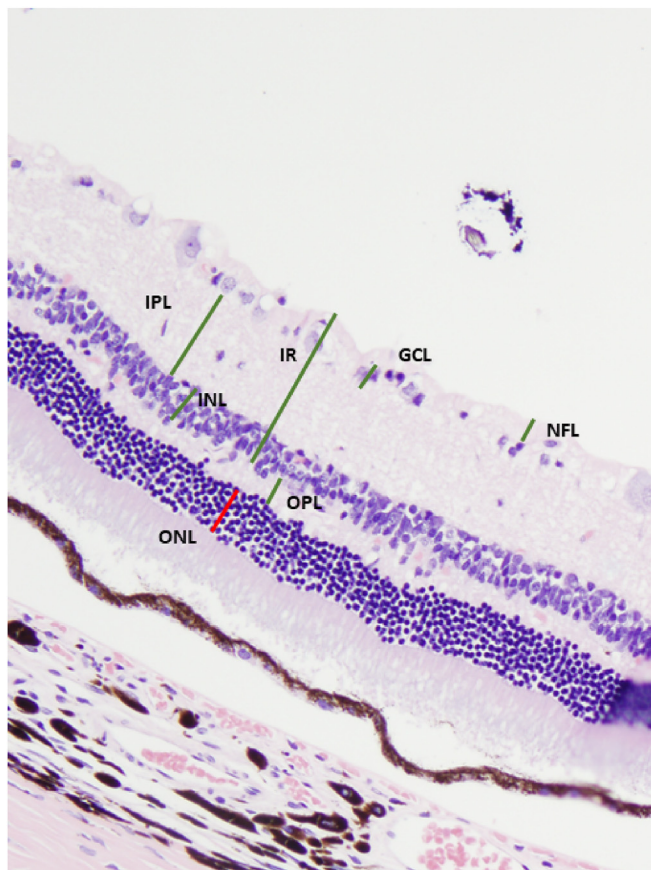


Fig. 2. Example of a histologic measurements of the retinal layers on the muskrat. ONL: outer nuclear layer, OPL: outer plexiform layer, IR: inner retina, INL: inner nuclear layer, IPL: inner plexiform layer, GCL: ganglion cell layer, NFL: nerve fiber layer.

diluted with deionized water (Amuno et al., 2018). The samples were then analyzed using a Varian ICP for the selected trace metals, where the quality control (QC) for the digestion was 15% for each batch for the selected elements, which included the use of in-house controls, duplicates and certified reference materials. An additional QC was performed as part of the instrumental analysis to ensure quality in the areas of instrumental drift.

Plants were washed prior to analysis to remove dust load on the plant samples. Trace elements were determined (VG101 package, ACME laboratories, Vancouver) in the vegetation samples using a 1 g split digested in nitric acid followed by Aqua Regia and analyzed by inductively coupled plasma mass spectrometry (ICP-MS). Vegetation samples were dried and macerated, and subsequently digested in aqua regia at 95 °C for 2 h, and with the resultant sample solutions diluted and analyzed by ICP-MS. A control reference material (CRM) was inserted after every 10th sample. ACME also inserted their own vegetation CRM samples after every 20th sample. Reagent blanks were used to correct instrument readings. The detection limits for As and Cd for soils and vegetation were 0.01 mg/kg and 0.001 mg/kg, respectively. Water samples were also collected from the muskrat sampling sites and analyzed for total As and Cd using graphite furnace atomic absorption spectrometer (AAAnalyst 800, PerkinElmer, USA). For surface water samples, a certified reference material (SLRS-6; National Research Council, Canada) was also analyzed to validate the efficiency of the applied method. The detection limit for water samples were 0.01 and 0.05 µg/L for Cd and As, respectively.

2.5. Statistical analysis

Independent samples *t*-test were used to compare the differences in retinal layer thicknesses of muskrats and squirrels collected from the mine area, intermediate location and the reference site (Tables 2 and 3). Furthermore, As and Cd content in surface soil, vegetation, surface water, and animals collected from the three sites were also compared. If normality assumptions were not met, different sites were compared with Mann-Whitney Rank Sum Test. A two-tailed Pearson correlation was employed to assess the relationships between As levels in the nails and retina layer parameters. The correlation analysis was not performed between nail Cd levels and retina layer parameters because the Cd levels were below detection limit in the nails of both muskrats and squirrels (Table 1) (also discussed in Amuno et al., 2019a, 2019b). The assumptions of normality of distribution and homogeneity of variances were verified with Shapiro-Wilk and Levene's tests, respectively. The sample size 'n' indicates the number of independent measurements conducted on tissues collected from different animals. A p-value of ≤ 0.05 was considered to be statistically significant. T-test comparisons were carried out in SigmaPlot 11 (Systat Software Inc., USA), boxplot figures were created using the ggplot package in R software version 3.1.2 (R Development Core Team, 2015; Wickham 2016) and correlation plots were created using corrplot package in R (Wei and Simko, 2017). Data points falling lower than $Q1 - (1.5 \times IQR)$ and higher than $Q3 + (1.5 \times IQR)$ for the boxplot analysis were considered outliers, where Q stands for quartile and IQR stands for inter-quartile range.

3. Results and discussions

3.1. Arsenic and cadmium exposure data

The environmental exposure data used in this study were derived from measurements of As and Cd in the nail samples of muskrats and red squirrels and other environmental samples (i.e. soil, surface water and vegetation samples) from the study area. The environmental samples exhibited nearly 10-fold higher concentrations for both metals at the mine site relative to the intermediate and reference sites (Table 1). Our previous studies have already reported elevated concentrations of As in the soils and vegetation samples from ~2 to 20 km radius of the vicinity of the Giant mine site (Amuno et al., 2018). In addition, a previous study conducted around 98 lakes within a 30 km radius of the City of Yellowknife already confirmed that As concentration exceeded the federal drinking water guideline of 10 µg/L for many lakes within 12 km of the Giant mine area (Palmer et al., 2015). In this present study, total arsenic (As) levels in the nails of muskrats and squirrels from arsenic contaminated areas were higher than those from the control areas. For example, the muskrats sampled from ~2 km radius of the mine area showed nail arsenic levels that ranged from 0.66 µg/g to 2.1 µg/g, which was in the range of 4.2–23 times higher than those from the reference site (i.e. below detection limit to 0.063 µg/g) approximately ~53.4 km–62 km away from Yellowknife. The maximum concentration of As in the nails of muskrats sampled from the intermediate location (~20 km) near the mine area was 3.02 µg/g, which was 47.6 times higher than the maximum concentration (0.063 µg/g) observed in reference muskrats. Possible explanation for why intermediate site concentration in one animal was being greater than mine site concentrations may be due to several factors such as changes in home range and elemental variation in the feeding habitats.

Cd was generally below the detection limit in the nails of muskrats and squirrels from the As affected areas as well as the reference area, suggesting that the animals from the study area

Table 1
Measured concentrations of As and Cd in nails of animals, surface soils, vegetation, and water from three different sites near mining area labelled as reference site, intermediate site (~20 KM from mine), and mine site (within ~2 KM radius). Within a parameter, different alphabets (superscripts) among the three sites indicate statistically significant difference ($p < 0.05$).

Site	Surface soils (mg/Kg dw) N = 36		Vegetation (mg/kg dw) N = 43		Water ($\mu\text{g/L}$) N = 12		Muskrat nails (mg/kg) N = 15		Squirrel nails (mg/kg) N = 15	
	As	Cd	As	Cd	As	Cd	As	Cd	As	Cd
Mine	74.6–400.2 ^A	0.2–0.7 ^A	21.9–727.2 ^A	0.04–1.13 ^A	110.3–213.6 ^A	<0.01	0.66–2.1 ^A	<0.01	<0.05–1.4 ^A	<0.01
Intermediate	0.6–54.3 ^B	<0.01–0.8 ^A	0.2–7.8 ^B	<0.001–1.13 ^{AB}	10.14–23.58 ^B	<0.01	<0.063–3.02 ^A	<0.01	<0.05–0.2 ^B	<0.01
Reference	0.9–10.3 ^C	<0.01–0.7 ^A	<0.001–0.6 ^C	0.34–3.15 ^{AC}	<0.05 ^C	<0.01	<0.05–0.063 ^B	<0.01	<0.05 ^B	<0.01

Symbol < indicates below detection limits.

N = total number of samples.

Table 2
Muskrat retina parameters values and statistical comparison with t-tests between mining site, intermediate site and a reference site. Analysis is reported as $t(\text{df}) = ; p =$ for parametric tests, with only the p value reported if a non-parametric Mann-Whitney U test was used (i.e. if the assumptions of normality or equal variance between sites were not met). * indicates significant difference at the level.

Parameter	Site	Length average \pm SEM (uM)	Statistical analysis		
			Mine vs Intermediate	Mine vs Reference	Intermediate vs Reference
ONL	Mine	48.38 \pm 4.9	$t(9) = 0.397; p = 0.701$	$t(8) = 0.244; p = 0.814$	$t(9) = 0.252; p = 0.807$
	Intermediate	41.96 \pm 5.09			
	Reference	43.48 \pm 2.35			
OPL	Mine	16.15 \pm 0.58	$t(8) = 0.144; p = 0.889$	$t(7) = 0.855; p = 0.421$	$t(9) = 0.366; p = 0.723$
	Intermediate	15.88 \pm 1.87			
	Reference	17.85 \pm 1.25			
INL	Mine	25.02 \pm 2.02	$t(9) = 1.031; p = 0.329$	$t(8) = 0.278; p = 0.788$	$t(9) = 1.315; p = 0.221$
	Intermediate	21.26 \pm 2.85			
	Reference	25.69 \pm 1.3			
IPL	Mine	53.65 \pm 4.32	$t(9) = 0.0434; p = 0.966$	$t(8) = 1.632; p = 0.141$	$t(9) = 1.044; p = 0.324$
	Intermediate	53.23 \pm 8.07			
	Reference	63.28 \pm 4.02			
GCL	Mine	14.36 \pm 1.58	$t(9) = 1.844; p = 0.098$	$t(8) = 2.564; p = 0.033^*$	$t(9) = 0.705; p = 0.499$
	Intermediate	19.23 \pm 2.01			
	Reference	21.34 \pm 2.22			
NFL	Mine	12.32 \pm 1.56	$t(3) = 0.866; p = 0.450$	$t(3) = 3.359; p = 0.044^*$	$p = 0.333$
	Intermediate	13.8 \pm 0.61			
	Reference	18.93 \pm 1.45			
IR	Mine	100.43 \pm 3.85	$t(9) = 0.0496; p = 0.962$	$t(8) = 2.752; p = 0.025^*$	$t(9) = 1.246; p = 0.244$
	Intermediate	99.66 \pm 13.68			
	Reference	119.59 \pm 5.81			

Table 3
Squirrel retina parameters compared with t-tests between mining site, intermediate site and a reference site. Analysis is reported as $t(\text{df}) = ; p =$ for parametric tests, with only the p value reported if a non-parametric Mann-Whitney U test was used (i.e. if the assumptions of normality or equal variance between sites were not met).

Parameter	Site	Length average \pm SEM (uM)	Statistical analysis		
			Mine vs Intermediate	Mine vs Reference	Intermediate vs Reference
ONL	Mine	19.41 \pm 1.29	$t(29) = -1.762; p = 0.089$	$t(24) = -2.586; p = 0.016^a$	$t(25) = -0.628; p = 0.536$
	Intermediate	23.95 \pm 2.19			
	Reference	26.04 \pm 2.44			
OPL	Mine	16.99 \pm 0.85	$p = 0.707$	$t(24) = -1.893; p = 0.071$	$t(25) = -1.838; p = 0.078$
	Intermediate	16.83 \pm 1.04			
	Reference	20.11 \pm 1.55			
INL	Mine	52.27 \pm 3.71	$p = 0.737$	$t(24) = -0.632; p = 0.533$	$p = 0.444$
	Intermediate	54.38 \pm 5.18			
	Reference	55.92 \pm 4.49			
IPL	Mine	73.76 \pm 3.94	$p = 0.185$	$p = 1$	$t(25) = -1.293; p = 0.208$
	Intermediate	67.37 \pm 4.03			
	Reference	75.78 \pm 5.22			
GCL	Mine	29.16 \pm 2.46	$p = 0.101$	$t(24) = 0.129; p = 0.898$	$t(25) = -1.465; p = 0.155$
	Intermediate	24.20 \pm 1.97			
	Reference	28.71 \pm 2.35			
NFL	Mine	52.47 \pm 5.11	$p = 0.621$	$t(24) = -0.912; p = 0.371$	$p = 0.711$
	Intermediate	55.05 \pm 8.1			
	Reference	45.51 \pm 5.55			
IR	Mine	211.12 \pm 12.57	$p = 0.313$	$p = 0.716$	$p = 0.711$
	Intermediate	202.84 \pm 11.94			
	Reference	210.3 \pm 13.27			

^a Indicates significant difference at alpha value of 0.05.

have not been chronically exposed to elevated levels of Cd in their home range and habitat. Total As concentration in the nails ranged from below detection limit to 1.4 $\mu\text{g/g}$ for squirrels sampled from ~ 2 km, but ranged from below detection limit to 0.2 $\mu\text{g/g}$ for the squirrels from the intermediate location 20 km, and was generally below detection limit in all the squirrel samples from the background location approximately 95–105 km away from Yellowknife.

3.2. Retina layer data

Results of the measurements of retinal layers are presented in Figs. 3 and 4. An independent *t*-test ($\alpha = 0.05$) was further conducted to compare the statistical differences between the three locations, with respect to retina layer changes (Tables 2 and 3).

3.2.1. Muskrats

In terms of measurement results, GCL thickness ranged from 10.3 μm to 19.2 μm for the muskrats closest to the vicinity of the Giant mine (~ 2 km), while that from the intermediate location ranged from 12.64 μm to 27.16 μm ; and 13.7 μm –26.8 μm for the reference area. Thicknesses of NFL ranged from 10.5 μm to 14.8 μm in the muskrats closest to the mine area, while that from the intermediate location was between 13.1 μm and 14.4 μm ; and 17.5 μm –20.4 μm for the muskrats from the background area. The thicknesses of the inner retina (IR) ranged from 89.1 μm to 112 μm in the muskrats closest to the mine, while that from the intermediate location ranged from 53.4 μm to 142.8 μm , and that from the reference area ranged from 106 μm to 138 μm . IPL ranged from 40.8 to 62.2 in muskrats closest to the mine area, while that from the intermediate location was between 21.4 μm and 80 μm ; and 55.2 μm –77.5 μm for the muskrats from the background area. Thickness of INL ranged from 19 μm to 30.8 μm in muskrats closest to the mine area, while that from the intermediate location was between 9.8 μm and 29.1 μm ; and 22.3 μm –30 μm for the muskrats from the background area. OPL ranged from 15.5 μm to 17.8 μm in muskrats closest to the mine area, while that from the intermediate location was between 9.1 μm and 22.1 μm ; and

14.5 μm –21.5 μm for the muskrats from the background area.

ONL ranged from 38.7 μm to 62.6 μm in muskrats closest to the mine area, while that from the intermediate location was between 29 μm and 58.3 μm ; and 36.7 μm –50.7 μm for the muskrats from the background area.

Inter-group comparisons of muskrats (Table 2) using *t*-test revealed that the thicknesses of GCL, NFL, and IR in muskrats were significantly different between the area closest to the mine (~ 2 km) and the background area (p values 0.033, 0.044, and 0.025 for GCL, NFL, and IR, respectively). We also noted that the thicknesses of GCL, IPL, NFL and IR were more reduced in the muskrats collected from the arsenic affected areas compared to the background site, although they were not statistically significant (Fig. 3A, C, D, G and Table 2). We also observed that ONL was relatively thicker in the muskrats from the mine area compared to the intermediate and reference location but it was not statistically different (p = 0.701 and 0.814, respectively) (Fig. 3E and Table 2).

3.2.2. Red squirrels

The thicknesses of NFL in samples from the mine area ranged from 20.6 μm to 79.6 μm , while that from the intermediate location ranged from 21.79 μm to 130.5 μm , and the reference site from 23.43 μm to 82.57 μm . The thicknesses of the inner retina (IR) of samples closest to the mine ranged from 142.2 μm to 254.5 μm , while that from the intermediate location was 144.5 μm –307.2 μm , and reference site from 160.8 μm to 301.5 μm . GCL thickness ranged from 14.5 μm to 48.5 μm , while that from the intermediate location ranged from 13.6 μm to 45 μm , and the reference site from 21.3 μm to 38.2 μm . IPL ranged from 60.9 μm to 81.9 μm in samples from closest to the mine, while that from the intermediate location ranged from 42.7 μm to 103.6 μm , and the reference site from 52.1 μm to 106.9 μm . INL ranged from 42.6 μm to 74.5 μm for the samples collected closest to the mine, while that from the intermediate location ranged from 31.2 μm to 102.7 μm and the reference site from 39.1 μm to 74.7 μm . OPL ranged from 14.8 μm to 23.9 μm for the samples collected from nearest the mine, while that from the intermediate location ranged from 11.3 μm to 25.2 μm , and

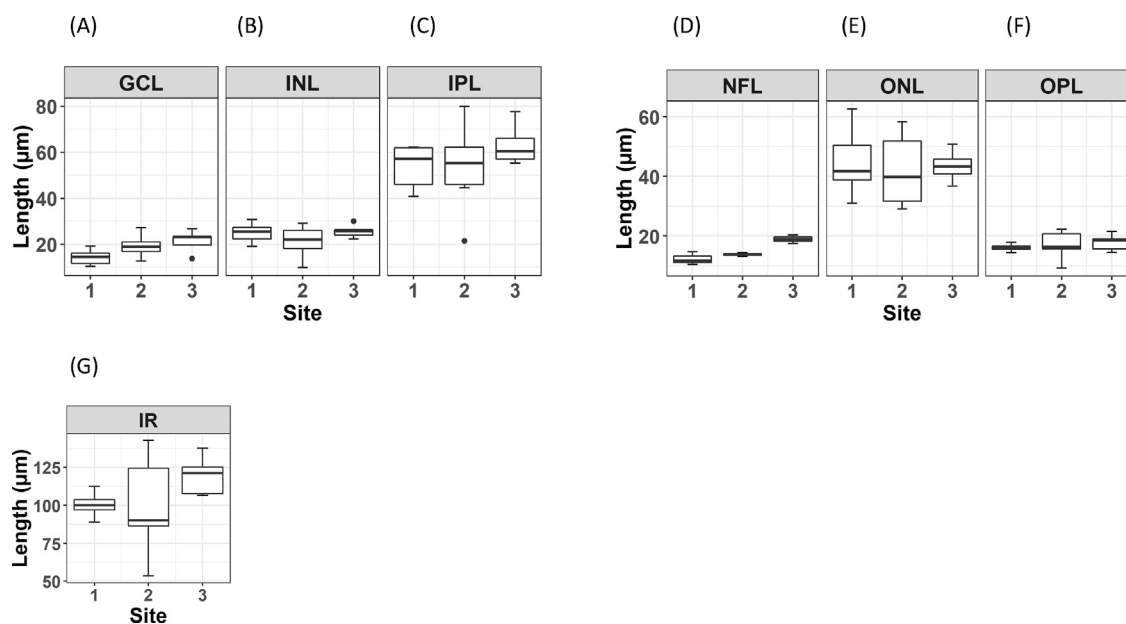


Fig. 3. Boxplots on the complete data for retinal layer changes in muskrats collected from three different sites, where site 3 represents reference site, site 2 represents intermediate location (~ 20 KM from mine), and site 1 represents locations in the vicinity of mine (within ~ 2 KM radius). The sample size (*n*) was 5–6 except NFL (*n* = 2–3). The closed circles represent outliers. The figure is subdivided into different panels with (A) GCL - Ganglion Cell Layer; (B) INL - Inner Nuclear Layer; (C) IPL - Inner Plexiform Layer; (D) NFL - Nerve Fibre Layer; (E) ONL - Outer Nuclear Layer; (F) OPL - Outer Plexiform Layer; (G) IR - Inner Retina Layer.

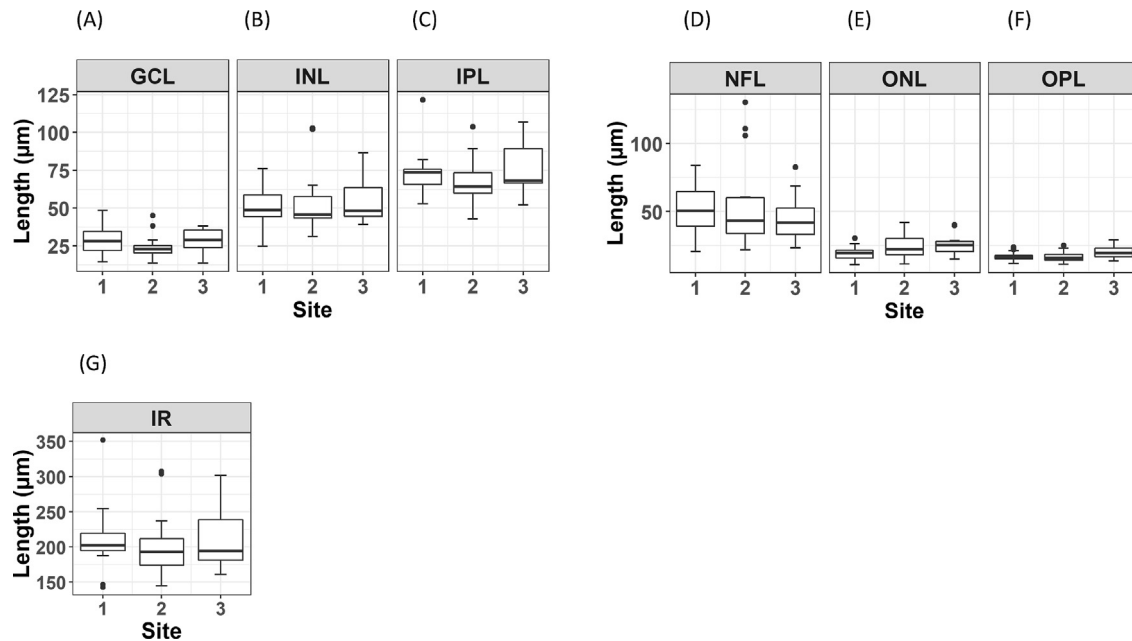


Fig. 4. Boxplots on the complete data for retinal layer changes in squirrels collected from three different sites, where site 3 represents reference site, site 2 represents intermediate location (~20 KM from mine), and site 1 represents locations in the vicinity of mine (within ~2 KM radius). The sample size (n) was 11–16. The closed circles represent outliers. The figure is subdivided into different panels with (A) GCL - Ganglion Cell Layer; (B) INL - Inner Nuclear Layer; (C) IPL - Inner Plexiform Layer; (D) NFL - Nerve Fibre Layer; (E) ONL - Outer Nuclear Layer; (F) OPL - Outer Plexiform Layer; (G) IR - Inner Retina Layer.

the reference location from 13.7 μm to 29.1 μm . ONL thickness ranged from 10.9 μm to 30.4 μm for the samples collected nearest the mine, while that from the intermediate location ranged from 11.3 μm to 41.9 μm , and the reference site from 15 μm to 28.6 μm . Inter-group comparisons (Table 3) using t -test revealed no statistical differences among the three groups for all the retina parameters except for ONL which showed a significant difference between the mine site and reference site ($p = 0.016$).

3.3. Correlation of retina parameters and contaminants

Correlation matrix revealed strong correlations between claw or nail arsenic content and different retina parameters for muskrats (Fig. 5), whereas no strong correlation was observed between the arsenic exposure data and retina layer changes in the squirrels (Fig. 6). In muskrats for example, nail arsenic concentration was found to be negative correlated with INL (-0.73), NFL (-0.95) and IR (-0.77), which suggest that chronic arsenic poisoning might be involved in inducing ganglion cell and axonal degeneration in the muskrats. Furthermore, the concentration of Cd in the guts of the muskrats was noted to be correlated with ONL (0.74). A negative correlation was observed between NFL thickness in muskrats and soil contamination with As (-0.64) and Cd (-0.72). Correlation matrix further showed a significant effect of distance on the NFL thickness of muskrats (0.88). The observed reduction in the thicknesses of GCL, NFL and IR in the muskrats from the mine site area and the intermediate location may be suggestive of neurodegeneration influenced by metal (loid) exposure. Although metal(loid) levels in nails have been used as biomarkers of exposures for humans in several studies (Mordukhovich et al., 2012; Nowak and Chmielnicka, 2000), the link is not well established in small mammals such as muskrats and squirrels. Therefore, it is very important to interpret the results with caution.

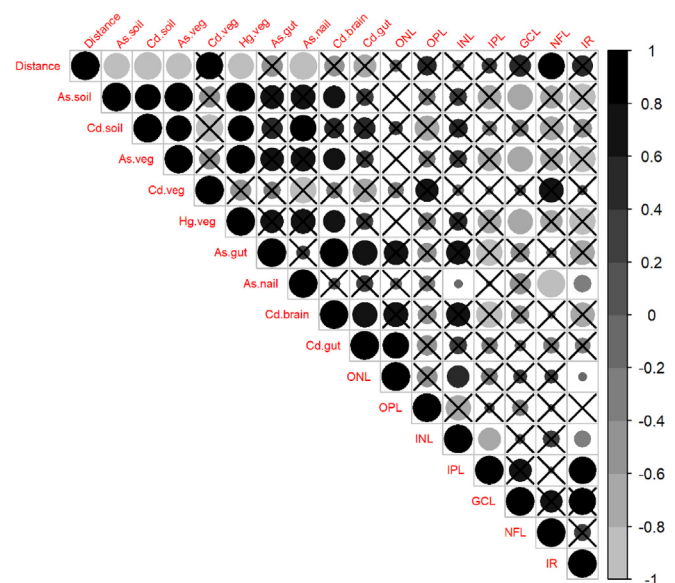


Fig. 5. Correlation between different parameters in muskrats. Positive correlation is depicted with blue colour and negative correlation is depicted with red colour. Correlations which are not significant at the 0.05 level are denoted as "X". In the figure, accumulation of arsenic (As) and cadmium (Cd) are shown in different compartments analyzed in this study (soil; vegetation (veg); brain; gut; nail). (For interpretation of colour in this figure legend, the reader is referred to the Web version of this article.)

3.4. Ocular histopathology

Tables 4 and 5 provide a summary of the kind of ocular lesions detected in squirrels and muskrats from the three different locations in response to arsenic contamination. Globes of muskrats from the vicinity of the mine site (~2 km) and in the intermediate location approximately 20 km from Yellowknife were all affected

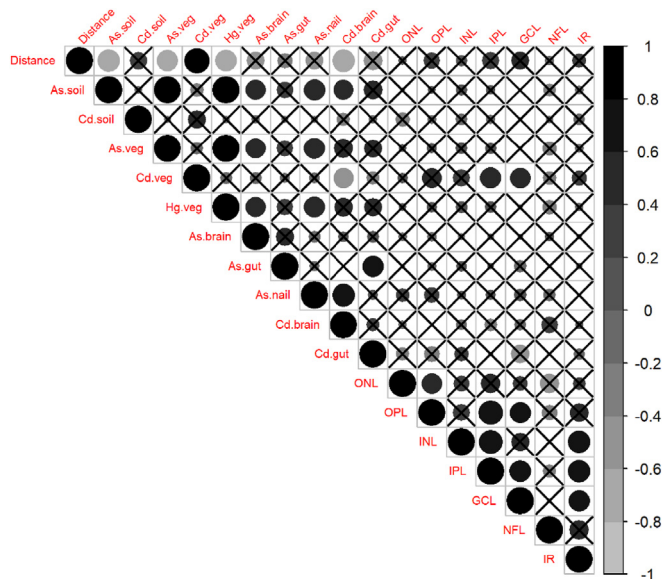


Fig. 6. Correlation between different parameters in squirrels. Positive correlation is depicted with blue colour and negative correlation is depicted with red colour. Correlations which are not significant at the 0.05 level are denoted as "X". In the figure, accumulation of arsenic (As) and cadmium (Cd) are depicted in different compartments analyzed in this study (soil; vegetation (veg); brain; gut; nail). (For interpretation of the references to colour in this figure legend, the reader is referred to the Web version of this article.)

Table 4
Histology lesions noted in Squirrels from the study area.

Lesion	Mine (~2 km)	Intermediate site (~20 km)	Reference site (~95–105 km)
Number of animals with lesions			
corneal scar	1	0	0
iris cyst	0	0	3

Table 5
Histology lesions noted in Muskrats from the study area.

Giant mine (~2 km)			
Sample ID	Right globe	Left globe	General remark
1	corneal vascularization (CV) and keratitis (K), and mild lymphocytic plasmacytic uveitis (LPU)	No abnormal findings (NAF)	
2	Unable to assess due to ocular damage	Retinal pigment epithelial hypertrophy (RPE) and retinal detachment, pigment dispersion, CV AND K, and LPU	Badly damaged eye with no retina, no lens, no iris to assess which may indicate previous ocular dehiscence and extrusion of contents.
3	mild K, mild LPU	CV and K, choroiditis	
4	CV and K	CV and K, moderate LPU	
5	mild LPU	CV and K and cataract	
Intermediate site (~20 km)			
1	cataract, mild CV and uveal cyst		
2	Mild LPU,	LPU, cataract, retinal degeneration and retinal detachment with RPE hypertrophy	
3	Mild LPU	Mild LPU	
4	LPU, CV and K	Mild LPU and uveal cyst	
5	LPU, cataract, CV and K	LPU	
Reference site (~53–62 km)			
51	Normal	Normal	
52	Mild LPU, CV and K	NAF	
53	NAF	NAF	
54	NAF	CV and K	
55	Mild LPU	LPU, CV and K	

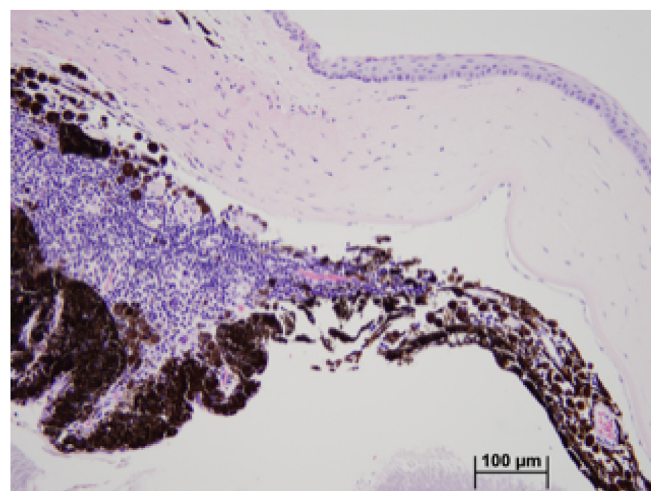


Fig. 7. These histologic sections of a muskrat eye from closest to the mine area (~2 km) reveals a marked iritis and cyclitis. The inflammatory cells are lymphocytes and plasma cells. Cornea is orientated at the top of each picture. (Hematoxylin and eosin stain).

with a moderate to marked lymphocytic plasmacytic uveitis (LPU) (Figs. 7 and 8) and vascularized keratitis (Fig. 9). Histologic examination of globes from the reference area, generally were without histologically identified lesions except for one muskrat with bilateral mild LPU, one with a mild unilateral LPU and a third with only a mild bilateral keratitis and in this particular sample lymphocytic follicles were observed throughout and within the anterior uvea and these lesions were accompanied by a moderate to severe keratitis. One muskrat from the mine area and intermediate location had histologic confirmation of cataracts (Fig. 10). The inflammation ranged from moderate to severe and two globes were noted to be phthisical (atrophic globes) (Fig. 11) and this pathology would have rendered the affected muskrat blind. No evidence of lens opacification and uveitis were identified histologically in squirrels across locations, but cornea scars were observed in a few squirrels from the vicinity of the mine area and background area.

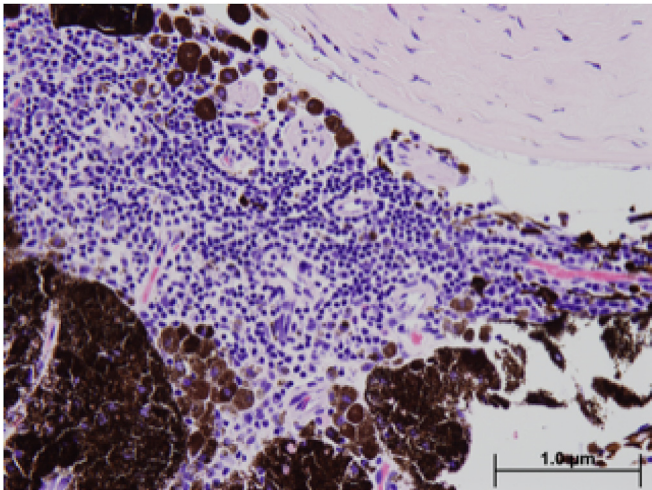


Fig. 8. These histologic sections of a muskrat eye from closest to the mine area (~2 km) reveals a marked iritis and cyclitis. The inflammatory cells are lymphocytes and plasma cells. Cornea is orientated at the top of each picture. (Hematoxylin and eosin stain).



Fig. 10. Metaplastic lens epithelium has migrated under the liquefied cortex along the posterior lens capsule in this muskrat from intermediate location (black arrow), and this pathology is consistent with cataract. (Periodic acid Schiff stain).

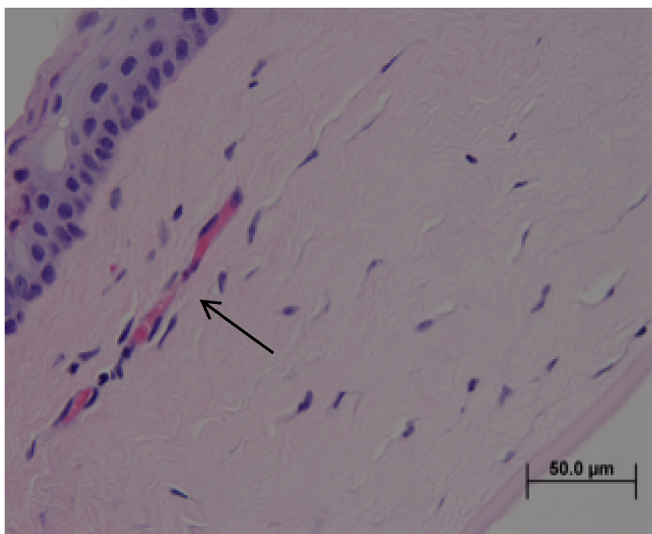


Fig. 9. This section of a muskrat cornea from intermediate location reveals corneal vascularization and fibrosis (black arrows) and a diffuse lymphocytic infiltrate (black arrows). (Hematoxylin and eosin stain).

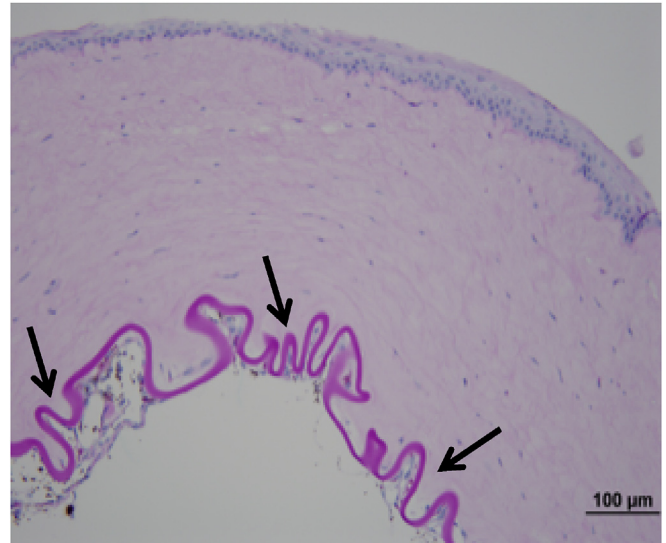


Fig. 11. Phthisis bulbi was noted in one muskrat from the mine area (~2 km). This section reveals the characteristic folding of Descemet's membrane (black arrows) that develops with an atrophic globe (phthisis bulbi). (Periodic acid Schiff).

In general, we note that retina layer changes were more prominent in the muskrats closest to the arsenic contaminated area near the mine area and intermediate location, and these areas have been previously identified, through current and previous investigation, to be significantly contaminated with high arsenic levels because of the previous gold mining activities and arsenopyrite mineralization (Amuno et al., 2018; Galloway et al., 2015; D'Entremont, 2014). The extent of and frequency of retina layer changes including the pattern of ocular lesions in the muskrats from the vicinity of the mine site and intermediate location were surprising, although we acknowledge that our sample sizes are extremely limited and no conclusion can be fully drawn at this stage. This is a wild population where ocular lesions would be expected to result in higher predation of the muskrats due to visual impairment or even blindness noted in some of these animals. Unfortunately, the pathogenesis of the ocular lesions is not known, although significant correlations between the inner retinal layers particularly ONL and NFL and Cd concentration within the

intestinal tracts, As content in nails, including As and Cd concentrations in the soils were observed. However, the LPU, cataracts and keratitis may or may not be related to these inner retinal changes or directly to the As and Cd exposure or even other causes including parasites or microbes. In general, the uveitis was severe in the muskrats from the arsenic affected areas. The loss of inner retinal layers noted histologically is most typical of glaucoma, and further field evaluations are needed to determine whether direct arsenic neurotoxicity or glaucoma secondary to uveitis was present. Glaucoma commonly develops secondary to uveitis and cataracts in animals.

Unfortunately, many infectious organisms and parasites, toxins, or chronic ocular injuries could also induce any or all of these lesions. Toxins such as zinc or lead or cadmium including arsenic exposure could be responsible for keratitis and cataract formation (See et al. 2007; Fabe et al., 2000; Shukla et al., 1964; Hallum, 1934) and the uveitis and glaucoma could have developed secondarily.

However, infections with organisms such as *Clostridium pilliformis* (Tyzzer's) (Chalmers and MacNeill, 1977), *Francisella tularensis* (Tuleremia) (Banfield, 1954; Ditchfield et al., 1960; Labzoffsky et al., 1952) *Yersinia pseudotuberculosis* or *Y. enterocolitica* (Yersiniosis) (Watson et al., 2001), are unreported and less likely infectious agents including *Toxoplasma congolensis* (Toxoplasmosis) or *Leptospira* (spp) (Leptospirosis) or *Giardia* (Giardiasis), and possible presence of others pathogens within these muskrats could be responsible for these uveitis which subsequently induced the keratitis, cataracts and secondary glaucoma.

Further investigations will be needed to rule out and identify the specific etiology and pathogenesis of these ocular lesions. Follow up studies are necessary in order to fully understand the possible roles of contaminants including infectious agents, uveitis and secondary glaucoma in causing these ocular damages. Uveitis is defined as inflammation of the iris, ciliary body, retina or choroid and it is the cause of legal blindness due to macular edema, and retina ischemia and secondary glaucoma. In some studies, uveitis can precede onset of neurological symptoms (Le Scanff et al., 2008; Curless and Bray, 1972). The frequency of co-existence of uveitis and CNS disease is suggested to be influenced from the common embryogenic development pathway of the posterior segment and CNS (Allegrì et al., 2011; Gordon and Goldstein, 2014). Uveitis is also associated with MS, and patients with uveitis masquerade with symptoms similar to MS (Messenger et al., 2015; Biousse et al., 1999). Humans with uveitis and neurological pathology are frequently diagnosed with Vogt–Koyanagi–Harada disease (Rao, 2007), central nervous system lymphoma (Coulon et al., 2002), or herpes virus infection (Sugita et al., 2008).

We had previously investigated the ocular pathology of snowshoe hares from the Yellowknife area exposed to arsenic and cadmium, but no specific ocular lesions were observed (Amuno et al., 2018). The muskrat is the first group of wild animals in the Yellowknife area that have demonstrated significant ocular disease in arsenic endemic areas, and we are puzzled at these unexpected findings and the potential significance. Firstly, muskrats that have these ocular lesions would likely be visually impaired which could make them more vulnerable to predation from owls, fox, wolves and mink. However, because muskrats are semi-aquatic rodents, it is likely that predators are somewhat less prevalent in their habitats or it is likely that the aquatic environment may have protected these affected animals from predation. Secondly, it is likely that the observed ocular lesions might be due to the effects of an infectious organism or the effects of chronic arsenic exposure or more likely both. We acknowledge that the sample size used in this study is relatively small and may affect confidence in the results and the generalization of the conclusions. To the best of our knowledge, the evidence presented in this study is the first preliminary investigation to describe the incidence and prevalence of ocular lesions in wildlife inhabiting arsenic endemic areas of Canada. The constellation of ocular abnormalities noted in the eyes of muskrats from the vicinity of the mine area suggests that ocular tissues may be targets for arsenic neurotoxicity.

4. Conclusion

We acknowledge that the sample size used in this study is relatively small and does not allow for the generalization of the conclusions. We also clarify that the limited dataset does not help to fully establish that arsenic contamination is the only factor responsible for causing ocular pathology in wildlife species in the study area, either at the population or individual levels. This study, to the best of our knowledge, is the first preliminary documentation of significant ocular pathology in wildlife from arsenic endemic areas of Canada. The results from this present study provide

baseline information regarding the effects of metal(loid)exposure on retino-neurologic pathology of muskrats and squirrels inhabiting the arsenic hot spot zones in Yellowknife. The preliminary results show that exposure to arsenic may be a contributing risk factor for the development of visual dysfunction in exposed muskrats. However, the test animals used in this study were caught from the field; hence, the possibility of infection with various organisms and parasites cannot be ruled out. These possible infectious agents may have the potential to cause ocular injuries observed in this study in both species. Hence, a follow-up study with possible infectious agents could be extremely useful in identifying the specific etiology and pathogenesis of the ocular lesions observed in this study. Nonetheless, the results reported in this study may serve as a sensitive indicator for assessing and monitoring the long-term effects of chronic arsenicosis and metal exposure in selected species of small mammal population in the Yellowknife environment.

Acknowledgments

Dr. Amuno is an adjunct professor at the School of Environment and Sustainability, and his participation in this study was undertaken independently and apart from his current work with the Nunavut Impact Review Board (NIRB). The analysis and views expressed in the study remain solely those of the authors and do not constitute the views of NIRB.

References

- Allegrì, P., Rissotto, R., Herbot, C.P., Murialdo, U., 2011. CNS diseases and uveitis. *J. Ophthalmic Vis. Res.* 6 (4), 284.
- Amuno, S., Jamwal, A., Grah, B., Niyogi, S., 2018. Chronic arsenicosis and cadmium exposure in wild snowshoe hares (*Lepus americanus*) breeding near Yellowknife, Northwest Territories (Canada), part 1: Evaluation of oxidative stress, antioxidant activities and hepatic damage. *Sci. Total Environ.* 618, 916–926.
- Amuno, S., Rudko, D.A., Gallino, D., Tuznik, M., Shekh, K., Kodzhahinchev, V., Niyogi, S., Chakravarty, M.M., Devenyi, G.A., 2019b. Altered neurotransmission and neuroimaging biomarkers of chronic arsenic poisoning in wild muskrats (*Ondatra zibethicus*) and red squirrels (*Tamiasciurus hudsonicus*) breeding near the City of Yellowknife, Northwest Territories (Canada). *Sci. Total Environ.* 30, 2019. November.
- Amuno, S., Shekh, K., Kodzhahinchev, V., Niyogi, S., 2019a. Neuropathological changes in wild muskrats (*Ondatra zibethicus*) and red squirrels (*Tamiasciurus hudsonicus*) breeding in arsenic endemic areas of Yellowknife, Northwest Territories (Canada): arsenic and cadmium accumulation in the brain and biomarkers of oxidative stress. *Sci. Total Environ.* 135426. November.
- Banfield, A.W.F., 1951. Notes on the mammals of the Mackenzie district, Northwest Territories. *Arctic Journal of The Arctic Institute of North America* 4 (2), 73–144.
- Banfield, A.W.F., 1954. Tularemia in beavers and muskrats, Waterton Lakes National Park, Alberta, 1952–53. *Can. J. Zool.* 32 (3), 139–143.
- Biousse, V., Trichet, C., Bloch-Michel, E., Roulet, E., 1999. Multiple sclerosis associated with uveitis in two large clinic-based series. *Neurology* 52 (1), 179–179.
- Bromstad, M.J., Wrye, L.A., Jamieson, H.E., 2017. The characterization, mobility, and persistence of roaster-derived arsenic in soils at giant mine, NWT. *Appl. Geochem.* 82, 102–118.
- Chalmers, G.A., MacNeill, A.C., 1977. Tyzzer's disease in wild-trapped muskrats in British Columbia. *J. Wildl. Dis.* 13 (2), 114–116.
- Chan, V.T., Tso, T.H., Tang, F., Tham, C., Mok, V., Chen, C., Wong, T.Y., Cheung, C.Y., 2017. Using retinal imaging to study dementia. *JoVE* 129, e56137.
- Clark, I.D., Raven, K.G., 2004. Sources and circulation of water and arsenic in the giant mine, Yellowknife, NWT, Canada. *Isot. Environ. Health Stud.* 40 (2), 115–128.
- Costello, F., Burton, J.M., 2018. Retinal imaging with optical coherence tomography: a biomarker in multiple sclerosis? *Eye Brain* 10, 47.
- Cott, P.A., Zajdlík, B.A., Palmer, M.J., McPherson, M.D., 2016. Arsenic and mercury in lake whitefish and burbot near the abandoned giant mine on Great Slave Lake. *J. Great Lake Res.* 42 (2), 223–232.
- Coulon, A., Lafitte, F., Hoang-Xuan, K., Martin-Duverneuil, N., Mokhtari, K., Blustajn, J., Chiras, J., 2002. Radiographic findings in 37 cases of primary CNS lymphoma in immunocompetent patients. *Eur. Radiol.* 12 (2), 329–340.
- Curless, R.G., Bray, P.F., 1972. Uveitis and multiple sclerosis in an adolescent. *Am. J. Dis. Child.* 123 (2), 149–150.
- D'Entremont, M., 2014. The presence of muskrats (*Ondatra zibethicus*) in a highly contaminated watershed near Yellowknife, Northwest Territories. *Northwest Nat.* 95, 113–115.
- DeSousa, E.A., Albert, R.H., Kalman, B., 2002. Cognitive impairments in multiple

- sclerosis: a review. *Am. J. Alzheimer's Dis. Other Dementias* 17 (1), 23–29.
- Ditchfield, J., Meads, E.B., Julian, R.J., 1960. Tularemia of muskrats in Eastern Ontario. *Canadian Journal of Public Health/Revue Canadienne de Sante'e Publique* 51 (12), 474–478.
- Dobson, R., Giovannoni, G., 2019. Multiple sclerosis—a review. *Eur. J. Neurol.* 26 (1), 27–40.
- Fabe, J.S., Grahn, B.H., Paterson, P.G., 2000. Zinc concentration of selected ocular tissues in zinc-deficient rats. *Biol. Trace Elem. Res.* 75 (1–3), 43–52.
- Fawcett, S.E., Jamieson, H.E., Nordstrom, D.K., McCleskey, R.B., 2015. Arsenic and antimony geochemistry of mine wastes, associated waters and sediments at the giant mine, Yellowknife, Northwest Territories, Canada. *Appl. Geochem.* 62, 3–17.
- Fisher, J.B., Jacobs, D.A., Markowitz, C.E., Galetta, S.L., Volpe, N.J., Nano-Schiavi, M.L., Baier, M.L., Frohman, E.M., Winslow, H., Frohman, T.C., 2006. Relation of visual function to retinal nerve fiber layer thickness in multiple sclerosis. *Ophthalmology* 113 (2), 324–332.
- Fukuoka, H., Nagaya, M., Toba, K., 2015. The occurrence of visual and cognitive impairment, and eye diseases in the super-elderly in Japan: a cross-sectional single-center study. *BMC Res. Notes* 8 (1), 619.
- Galloway, J.M., Palmer, M., Jamieson, H.E., Patterson, R.T., Nasser, N., Falck, H., Macumber, A.L., Goldsmith, S.A., Sanei, H., Normandeau, P., Hadlari, T., Roe, H.M., Nevile, L.A., Lemay, D., 2015. Geochemistry of lakes across eozones in the Northwest Territories and implications for the distribution of arsenic in the Yellowknife region. *Geological Survey of Canada, Open File* 7908, 1.
- Gordon, L.K., Goldstein, D.A., 2014. Gender and uveitis in patients with multiple sclerosis. *Journal of ophthalmology* 2014.
- Government of Northwest Territories, 2016. Concentrations of mercury and other heavy metals in furbearers from the Slave River. *Environmental Research Bulletin* 1 (3). https://www.enr.gov.nt.ca/sites/enr/files/128-cimp_bulletin_v1i3-proof.pdf.
- Grahn, B.H., Peiffer, R.L., Wilcock, B.W., 2018. *Histologic Basis of Ocular Disease in Animals*. Wiley Blackwell.
- Hallum, A.V., 1934. Involvement of the cornea in arsenic poisoning: report of a case. *Arch. Ophthalmol.* 12 (1), 93–98.
- Hutchinson, T.C., Aufreiter, S., Hancock, R.G.V., 1982. Arsenic pollution in the Yellowknife area from gold smelter activities. *J. Radioanal. Chem.* 71 (1–2), 59–73.
- Ikram, M.K., Cheung, C.Y., Wong, T.Y., Chen, C.P., 2012. Retinal pathology as biomarker for cognitive impairment and Alzheimer's disease. *J. Neurol. Neurosurg. Psychiatr.* 83 (9), 917–922.
- Iranzo, A., Molinuevo, J.L., Santamaría, J., Serradell, M., Martí, M.J., Valldeoriola, F., Tolosa, E., 2006. Rapid-eye-movement sleep behaviour disorder as an early marker for a neurodegenerative disorder: a descriptive study. *Lancet Neurol.* 5 (7), 572–577.
- Jefferis, J.M., Mosimann, U.P., Clarke, M.P., 2011. Republished review: cataract and cognitive impairment: a review of the literature. *Postgrad. Med.* 87 (1031), 636–642.
- Jung, N.-Y., Han, J.C., Ong, Y.T., Cheung, C.Y.-I., Chen, C.P., Wong, T.Y., Kim, H.J., Kim, Y.J., Lee, J., San Lee, J., 2019. Retinal microvasculature changes in amyloid-negative subcortical vascular cognitive impairment compared to amyloid-positive Alzheimer's disease. *J. Neurol. Sci.* 396, 94–101.
- Karussis, D., 2014. The diagnosis of multiple sclerosis and the various related demyelinating syndromes: a critical review. *J. Autoimmun.* 48, 134–142.
- Kesler, A., Vakhapova, V., Korczyn, A.D., Naftaliev, E., Neudorfer, M., 2011. Retinal thickness in patients with mild cognitive impairment and Alzheimer's disease. *Clin. Neurol. Neurosurg.* 113 (7), 523–526.
- Kobayashi, Y., Agusa, T., 2019. *Arsenic Metabolism and Toxicity in Humans and Animals: Racial and Species Differences*. *Arsenic Contamination in Asia*. Springer, pp. 13–28.
- Kwapong, W.R., Ye, H., Peng, C., Zhuang, X., Wang, J., Shen, M., Lu, F., 2018. Retinal microvascular impairment in the early stages of Parkinson's disease. *Invest. Ophthalmol. Vis. Sci.* 59 (10), 4115–4122.
- Labzoffsky, N.A., Sprent, J.A.F., 1952. Tularemia among beaver and muskrat in Ontario. *Can. J. Med. Sci.* 30 (3), 250–255.
- Le Scannf, J., Sève, P., Renoux, C., Broussolle, C., Confavreux, C., Vukusic, S., 2008. Uveitis associated with multiple sclerosis. *Multiple Sclerosis Journal* 14 (3), 415–417.
- London, A., Benhar, I., Schwartz, M., 2013. The retina as a window to the brain—from eye research to CNS disorders. *Nat. Rev. Neurol.* 9 (1), 44.
- McKeith, I.G., Dickson, D., Lowe, J., Emre, M., O'Brien, J., Feldman, H., Cummings, J., Duda, J., Lippa, C., Perry, E., 2005. Diagnosis and management of dementia with Lewy bodies third report of the DLB consortium. *Neurology* 65 (12), 1863–1872.
- Messenger, W., Hildebrandt, L., Mackensen, F., Suhler, E., Becker, M., Rosenbaum, J.T., 2015. Characterisation of uveitis in association with multiple sclerosis. *Br. J. Ophthalmol.* 99 (2), 205–209.
- Miller, D., Barkhof, F., Montalban, X., Thompson, A., Filippi, M., 2005. Clinically isolated syndromes suggestive of multiple sclerosis, part I: natural history, pathogenesis, diagnosis, and prognosis. *Lancet Neurol.* 4 (5), 281–288.
- Moller, H., 1983. Foods and foraging behaviour of Red (*Sciurus vulgaris*) and Grey (*Sciurus carolinensis*) squirrels. *Mamm. Rev.* 13, 81–98.
- Mordukhovich, I., Wright, R.O., Hu, H., Amarasiriwardena, C., Baccarelli, A., Litonjua, A., Sparrow, D., Vokonas, P., Schwartz, J., 2012. Associations of toenail arsenic, cadmium, mercury, manganese, and lead with blood pressure in the normative aging study. *Environ. Health Perspect.* 120 (1), 98–104.
- New York department of environmental conservation. <https://www.dec.ny.gov/animals/57561.html>.
- Nowak, B., Chmielnicka, J., 2000. Relationship of lead and cadmium to essential elements in hair, teeth, and nails of environmentally exposed people. *Ecotoxicol. Environ. Saf.* 46, 265–274.
- O'Brien, D.J., Kaneene, J.B., Poppenga, R.H., 1993. The Use of Mammals as Sentinels for Human exposure to toxic contaminants in the environment. *Environmental Health Perspectives* 99, 351–368.
- Palmer, M.J., Galloway, J.M., Jamieson, H.E., Patterson, R.T., Falck, H., Kokelj, S.V., 2015. The concentration of arsenic in lake waters of the Yellowknife area; Northwest Territories Geological Survey, NWT Open File 2015-06.
- Parisi, V., Manni, G., Spadaro, M., Colacino, G., Restuccia, R., Marchi, S., Bucci, G., Pierelli, F., 1999. Correlation between morphological and functional retinal impairment in multiple sclerosis patients. *Invest. Ophthalmol. Vis. Sci.* 40 (11), 2520–2527.
- Pennsylvania State University (2002). *The Virtual Nature Trail at Penn State New Kensington*. <https://www.psu.edu/dept/nkbiology/naturetrail/speciespages/redquirrel.htm>.
- R Development Core Team, 2015. *R: A Language and Environment for Statistical Computing*. R Foundation for Statistical Computing, Vienna.
- Rao, N.A., 2007. Pathology of vogt–koyanagi–harada disease. *Int. Ophthalmol.* 27 (2–3), 81–85.
- Ruff, S., Wilson, D., 1999. *The Smithsonian Book of North American Mammals*. Smithsonian Institution Press in association with the American Society of Mammalogists, Washington (D.C.).
- Saidha, S., Syc, S.B., Durbin, M.K., Eckstein, C., Oakley, J.D., Meyer, S.A., Conger, A., Frohman, T.C., Newsome, S., Ratchford, J.N., 2011. Visual dysfunction in multiple sclerosis correlates better with optical coherence tomography derived estimates of macular ganglion cell layer thickness than peripapillary retinal nerve fiber layer thickness. *Multiple Sclerosis Journal* 17 (12), 1449–1463.
- Satue, M., Obis, J., Rodrigo, M.J., Otin, S., Fuertes, M.I., Vilades, E., Gracia, H., Ara, J.R., Alarcia, R., Polo, V., 2016. Optical coherence tomography as a biomarker for diagnosis, progression, and prognosis of neurodegenerative diseases. *Journal of ophthalmology*, 2016.
- See, L.C., Chiou, H.Y., Lee, J.S., Hsueh, Y.M., Lin, S.M., Tu, M.C., Yang, M.L., Chen, C.J., 2007. Dose-response relationship between ingested arsenic and cataracts among residents in Southwestern Taiwan. *Journal of Environmental Science and Health Part A* 42 (12), 1843–1851.
- Shentu, Y.-P., Hu, W.-t., Zhang, Q., Huo, X., Liang, J.-W., Liuyang, Z.-Y., Zhou, H., Wei, H., Ke, D., Wang, X.-C., 2019. CIP2A-promoted astrogliosis induces AD-like synaptic degeneration and cognitive deficits. *Neurobiol. Aging* 75, 198–208.
- Shukla, B.R., Ahuja, O.P., Paul, S.D., 1964. Arsenical optic atrophy. *Indian J. Ophthalmol.* 12 (1), 15.
- Stearns, L., Goodwin, M., 1941. Notes on the winter feeding of the muskrat in Delaware. *J. Wildl. Manag.* 5 (1), 1–12.
- Sugita, S., Shimizu, N., Watanabe, K., Mizukami, M., Morio, T., Sugamoto, Y., Mochizuki, M., 2008. Use of multiplex PCR and real-time PCR to detect human herpes virus genome in ocular fluids of patients with uveitis. *Br. J. Ophthalmol.* 92 (7), 928–932.
- Wagemann, R., Snow, N.B., Rosenberg, D.M., Lutz, A., 1978. Arsenic in sediments, water and aquatic biota from lakes in the vicinity of Yellowknife, Northwest Territories, Canada. *Arch. Environ. Contam. Toxicol.* 7 (1), 169–191.
- Watson, R.P., Blanchard, T.W., Mense, M.G., Gasper, P.W., 2001. Histopathology of experimental plague in cats. *Vet. Pathol.* 38 (2), 165–172.
- Wei, T., Simko, V., 2017. *R Package "corrplot": Visualization of a Correlation Matrix*. Available from, Version 0.84. <https://github.com/taiyun/corrplot>.
- Woodland Fish and Wildlife, 2015. *Beaver, Muskrat, and Nutria on Small Woodlands A Guide to Understanding America's Largest Rodents*. <https://westernforestry.org/WoodlandFishAndWildlife/wp-content/uploads/2015/05/beaver.pdf>.